Histidine, Lysine, and Arginine Radical Cations: Isomer Control via the Choice of Auxiliary Ligand (L) in the Dissociation of [Cu II (L)(amino acid)] •2+ Complexes

ARTICLE *in* THE JOURNAL OF PHYSICAL CHEMISTRY B · JANUARY 2008

Impact Factor: 3.3 · DOI: 10.1021/jp0746648 · Source: PubMed

5 AUTHORS, INCLUDING:

Yuyong ke
Endoceutics inc, Canada
19 PUBLICATIONS **298** CITATIONS

Histidine, Lysine, and Arginine Radical Cations: Isomer Control via the Choice of Auxiliary Ligand (L) in the Dissociation of $[Cu^{II}(L)(amino\ acid)]^{\bullet 2+}$ Complexes

Yuyong Ke, Junfang Zhao, Udo H. Verkerk, Alan C. Hopkinson, and K. W. Michael Siu*

Department of Chemistry and Centre for Research in Mass Spectrometry, York University, 4700 Keele Street, Toronto, Ontario, Canada M3J 1P3

Received: June 15, 2007; In Final Form: October 4, 2007

Histidine, lysine, and arginine radical cations have been generated through collision-induced dissociation (CID) of complexes $[Cu^{II}(auxiliary\ ligand)_n(amino\ acid)]^{\bullet 2+}$, using tri-, bi-, as well as monodentate auxiliary ligands. On the basis of the observed CID products, the existence of two isomeric amino-acid populations is postulated. The Type 1 radical cations of histidine and lysine, stable on the mass spectrometer time scale, were found to lose water, followed by the loss of carbon monoxide under more energetic CID conditions. The arginine Type 1 radical cation behaved differently, losing dehydroalanine. The Type 2 radical cations were metastable and easily fragmented by the loss of carbon dioxide, effectively preventing direct observation. Type 1 radical cations are proposed to result from neutral (canonical) amino-acid coordination, whereas Type 2 radical cations are from zwitterionic amino-acid coordination to copper in the complex. The ratio of Type 1/Type 2 ions was found to be dependent on the auxiliary ligand, providing a method of controlling which radical cation would be formed primarily. Density functional calculations at B3LYP/6-311++G(d,p) have been used to determine the relative energies of five $His^{\bullet +}$ isomers. Barriers against interconversion between the isomers and against fragmentation have been calculated, giving insight as to why the Type 1 ions are stable, while only fragmentation products of the Type 2 ions are observable under CID conditions.

Introduction

The amino acids histidine, arginine, and lysine are known to have high affinities for divalent metal ions.[1−9] These residues are often featured prominently in the active sites of enzymes, regulating activity through variable coordination of the metal cofactor.[10−12] The involvement of histidine binding has been demonstrated for a number of copper-containing metalloproteins, including azurin[13] and superoxide dismutase.[14] To gain further understanding as well as to isolate the catalytic potential of such active sites, model systems have been used. Unfortunately, these often add unexpected complexity; a result of the large number of possible coordination modes of, for instance, histidine.[15,16] Soft ionization techniques (e.g., electrospray ionization (ESI)) enable the practice of mass spectrometry on metalloproteins and their corresponding models in the gas phase and in the absence of solvation effects. Recently, collision-induced dissociation (CID) of ternary complexes comprising Cu^{II}, diethylenetriamine (dien), and a peptide was shown to result in the generation of cationic peptide radicals that can be isolated and sequenced through further fragmentation using multiple stages of CID.[17−21]

This discovery opened a new opportunity to conducting gas-phase redox chemistry and developing the use of metal-peptide complexes as a source of analytically useful peptide ions. Efforts by our group[17−21] and others[22−31] have focused on investigating the influence of the metal[29] and auxiliary ligand[22,23,27] on the various and competing fragmentation pathways of the ternary complexes. The coordination mode of the amino acid or peptide to the copper may have an influence on its subsequent gas-phase fragmentation. The seminal work of Hu and Loo[32] on the CID behaviors of $Cu^{\bullet 2+}$, Zn^{2+}, Ni^{2+}, and $Co^{\bullet 2+}$/angiotensin complexes strongly suggests that $Cu^{\bullet 2+}$, in contrast to the other three metal ions, preferentially interacts with the C-terminal carboxyl group, thereby significantly increasing the loss of CO_2 in subsequent CID. This difference in CID behaviors was not evident in the dissociation of complexes containing the corresponding C-terminal amidated peptides. Barlow et al.[27] reported a "memory effect" observed in the dissociation of the peptide radical ions $TyrGlyGlyPheLeuArg^{\bullet +}$ formed from Cu^{II} ternary complexes containing the tridentate, 2,2′:6′,2″-terpyridine (tpy), and the bidentate, 3,4,7,8-tetramethyl-1,10-phenanthroline, as the auxiliary ligand. This memory effect manifested itself in drastically different CID spectra that were attributed to a difference in the way that the radical peptides were formed, which in turn might be a consequence of different peptide binding modes. Further studies on the influence of the basic residue (arginine, lysine, histidine) on fragmentation behaviors of tripeptides[30] and on the effect of different auxiliary ligands on the CID of ternary complexes containing amino acids[31] support this possibility.

Fragmentation pathways in a generic complex $[Cu^{II}(L)(M)]^{\bullet 2+}$ (where L is the auxiliary ligand and M is the peptide), all leading to the separation of charge, that have been observed are as follows:[17−31]

$$\text{Peptide radical formation: } [Cu^{II}(L)(M)]^{\bullet 2+} \rightarrow [Cu^{I}(L)]^{+} + M^{\bullet +} \quad (1)$$

$$\text{Proton addition to the peptide: } [Cu^{II}(L)(M)]^{\bullet 2+} \rightarrow [Cu^{II}(L-H)]^{\bullet +} + [M+H]^{+} \quad (2)$$

* Corresponding author. Address: Department of Chemistry and Centre for Research in Mass Spectrometry, York University, 4700 Keele Street, Toronto, Ontario, Canada M3J 1P3. Phone: (416)-650-8021. Fax: (416)-736-5936. E-mail: kwmsiu@yorku.ca.

10.1021/jp0746648 CCC: $37.00
Published on Web 12/06/2007

Proton abstraction from the peptide: $[Cu^{II}(L)(M)]^{\bullet 2+} \rightarrow [Cu^{II}(M - H)]^{\bullet +} + [L + H]^{+}$ (3)

Peptide fragmentation: $[Cu^{II}(L)(M)]^{\bullet 2+} \rightarrow [Cu^{II}(L)(M - b_n)]^{\bullet +} + b_n^{+}$ (4)

Here we report the formation of two different radical-cation types of histidine, lysine, and arginine generated by the CID of $[Cu^{II}(L)_n(M)]^{\bullet 2+}$ and show that the relative abundances of the two types are controlled by the auxiliary ligand. Amino-acid binding modes and fragmentation behavior of the histidine radical cation isomers are further investigated using density functional theory (DFT) calculations.

Experimental Section

Mass Spectrometry. Experiments were performed using a commercially available ion-trap mass spectrometer (Finnigan-MAT LCQ) equipped with an ESI source. The typical electrospray voltage was 4.5 kV. Nitrogen was used as the sheath gas at a flow rate of 0.3 L/min. The capillary temperature was 120−160 °C. The metal complexes were infused at a flow rate of 2−3 μL/min. Ion lineage was determined using the scan functions of an LCQ instrument.

Materials. Metal complexes were prepared in 1-mL 50/50 water/methanol solutions, by mixing copper(II) perchlorate, the auxiliary ligand 1,3,5-triazacyclononane (tacn), 2,2′-bipyridine (bpy) or tpy, and the amino acid histidine, lysine, or arginine to a final concentration of 100 μM $[Cu^{II}(\text{auxiliary ligand})(M)]^{\bullet 2+}$. In experiments where acetone was used as the auxiliary ligand, 1−5 vol % acetone was directly added to the metal/amino acid complex solution. Experiments without auxiliary ligand were 100 μM in $[Cu^{II}(M)_2]^{\bullet 2+}$. The amino acids, copper(II) perchlorate, auxiliary ligands, and solvents were purchased from Sigma (St. Louis, MO) and used without further purification. ^{15}N α-labeled L-lysine was purchased from Cambridge Isotope Laboratories; labeled α,β,β-d_3 DL-histidine was from CDN Isotopes, Pointe-Claire, Quebec, Canada.

Computational Method. Quantum chemical computations were performed using the Gaussian 03 suite of programs[33] with the hybrid DFT B3LYP model based on Becke's three-parameter exchange potential[34] and the Lee, Yang, and Parr correlation functional[35] with unrestricted orbitals. The geometries of the copper complexes were fully optimized in the gas phase using the standard Pople 6-311++G(d,p) basis set. Harmonic frequency calculations were used to characterize each critical point and to determine zero-point vibrational energies. No frequency scaling was applied. This level of theory has proved adequate for the study of copper ion/(poly)peptide interactions.[36−38] Every transition state structure for the isomerization and fragmentation of histidine radical cations was found and characterized by a single imaginary frequency. The reactants and products associated with each transition state structure were established using the intrinsic reaction coordinate method.[39]

Results and Discussion

Histidine. Figure 1 shows the results of gas-phase fragmentation of copper(II) complexes $[^{63}Cu^{II}(L)_n(M)]^{\bullet 2+}$ with $(L)_n$ being (a) dien, $n = 1$; (b) tacn, $n = 1$; (c) tpy, $n = 1$; (d) bpy, $n = 1$; (e) His (i.e., L = M = His); and (f) acetone, $n = 2$, all under a relative collision energy of 8%. (All spectra of Cu-containing ions shown hereon will be those of ^{63}Cu, unless specified otherwise.) It is apparent that at least two of the aforementioned dissociation channels were operative. In addition to dissociative electron transfer that led to the formation of $His^{\bullet +}$ and $[Cu^{I}(L)]^{+}$ (eq 1), varying degrees of the competing dissociative proton-transfer reaction occurred as well, leading to $[His + H]^{+}$ and $[Cu^{II}(L - H)]^{\bullet +}$ (eq 2). The use of tacn as L resulted in approximately equal abundances of $His^{\bullet +}$ and $[His + H]^{+}$ (although dissociative electron transfer was probably about 3 times more effective than dissociative proton transfer, as judged by the relative ratio of $[Cu^{I}(L)]^{+}$ to $[Cu^{II}(L - H)]^{\bullet +}$). In contrast, dissociative proton transfer is apparently absent in $(L)_n$ = tpy and bpy, (no $[His + H]^{+}$ and $[Cu^{II}(L - H)]^{\bullet +}$ in Figure 1c,d). The common CID products at 111 and 82 Th could not have been formed from the subsequent dissociation of $[His + H]^{+}$, as the latter results in fragments of 138 Th (the b_1 ion) and 110 Th (the a_1 ion) after sequential elimination of water and CO, respectively (Figure 2a). Lavanant et al.[39] observed fragment ions at 111 and 82 Th in the CID of $[Cu^{II}(His)_2]^{\bullet 2+}$; significantly, $His^{\bullet +}$ was absent, although its complementary ion, $[Cu^{I}(His)]^{+}$, was present abundantly. The 111 Th ion was proposed to form via the elimination of CO_2 from $His^{\bullet +}$, while the 82 Th ion was the protonated histidine side chain (see later). Thus, the 111 and 82 Th radical ions are attributed to $His^{\bullet +}$, fragmenting by the loss of CO_2 and, subsequently, $NH{=}CH_2$. In contrast, studies by Barlow et al.[31] on $[Fe^{III}(\text{salen})(His)]^{\bullet +}$ and $[Cu^{II}(\text{terpy})(His)]^{\bullet 2+}$complexes did not report losses of CO_2 (although the CID spectrum of the latter probably contains a peak at 111 Th at <5% abundance). Significantly, CID of *the isolated* $His^{\bullet +}$ *ion at 155 Th* in our experiments did not result in the loss of CO_2; instead, the loss of water occurred, forming the $[b_1 - H]^{\bullet +}$ ion at 137 Th, which in turn lost CO to form the $[a_1 - H]^{\bullet +}$ ion at 109 Th (Figure 2b), corroborating results obtained by Barlow et al.[31] Compared to the radical cation fragment ions 111 Th and 82 Th generated with L = tpy and tacn, these same fragments were found to be in higher abundances, relative to $His^{\bullet +}$ at 155 Th, with L = bpy (Figure 1d), histidine (Figure 1e), and acetone (Figure 1f). The CID of $[Cu^{II}(His)_2]^{\bullet 2+}$ in our experiments yielded a low abundance of $His^{\bullet +}$ at 155 Th (Figure 1e) along with an even lower abundance of $[His + H]^{+}$; CID of $[Cu^{II}(\text{acetone})_2(His)]^{\bullet 2+}$ yielded the characteristic fragmentation products at 111 and 82 Th (Figure 1f), but (practically) no $His^{\bullet +}$. The isolation and CID of the 111 Th fragment cleanly generated the 82 Th product ion; the neutral product that was eliminated contained one exchangeable hydrogen (Figure 3). The formation of a product of 82 Th from $[Cu^{II}(\text{tpy})(His)]^{\bullet 2+}$ has also been described by Barlow et al.[31] On the basis of experiments using methylated histidines and DFT calculations on a canonical histidine radical cation, these authors proposed a McLafferty-type rearrangement for generating the product at 82 Th. That proposal, however, did not take into account formation of the ion observed at 111 Th.

The dissociation spectra of $[Cu^{II}(L)_n(M)]^{\bullet 2+}$ shown above can readily be rationalized, if one hypothesizes that CID results in two populations of isomeric histidine radical cations having different stabilities on the mass spectrometer time scale. In the following discussion, the observed stable amino-acid radical cation is denoted Type 1, while the metastable radical cation that rapidly loses CO_2 is denoted Type 2 (see Scheme 1). The extent of the formation of Types 1 and 2 histidine radical cations can be modulated by the use of different auxiliary ligands. The use of *acetone* as an auxiliary ligand generates *almost exclusively the metastable Type 2 radical cation*, while the use of *tpy* generates *mainly the stable Type 1 radical cation*. Similar results have also been obtained with lysine and arginine.

Lysine and Arginine. The CID of $[Cu^{II}(L)(Lys)]^{\bullet 2+}$ (L = tacn, bpy, and lysine; Figure 4a, b, and c, respectively) exhibits

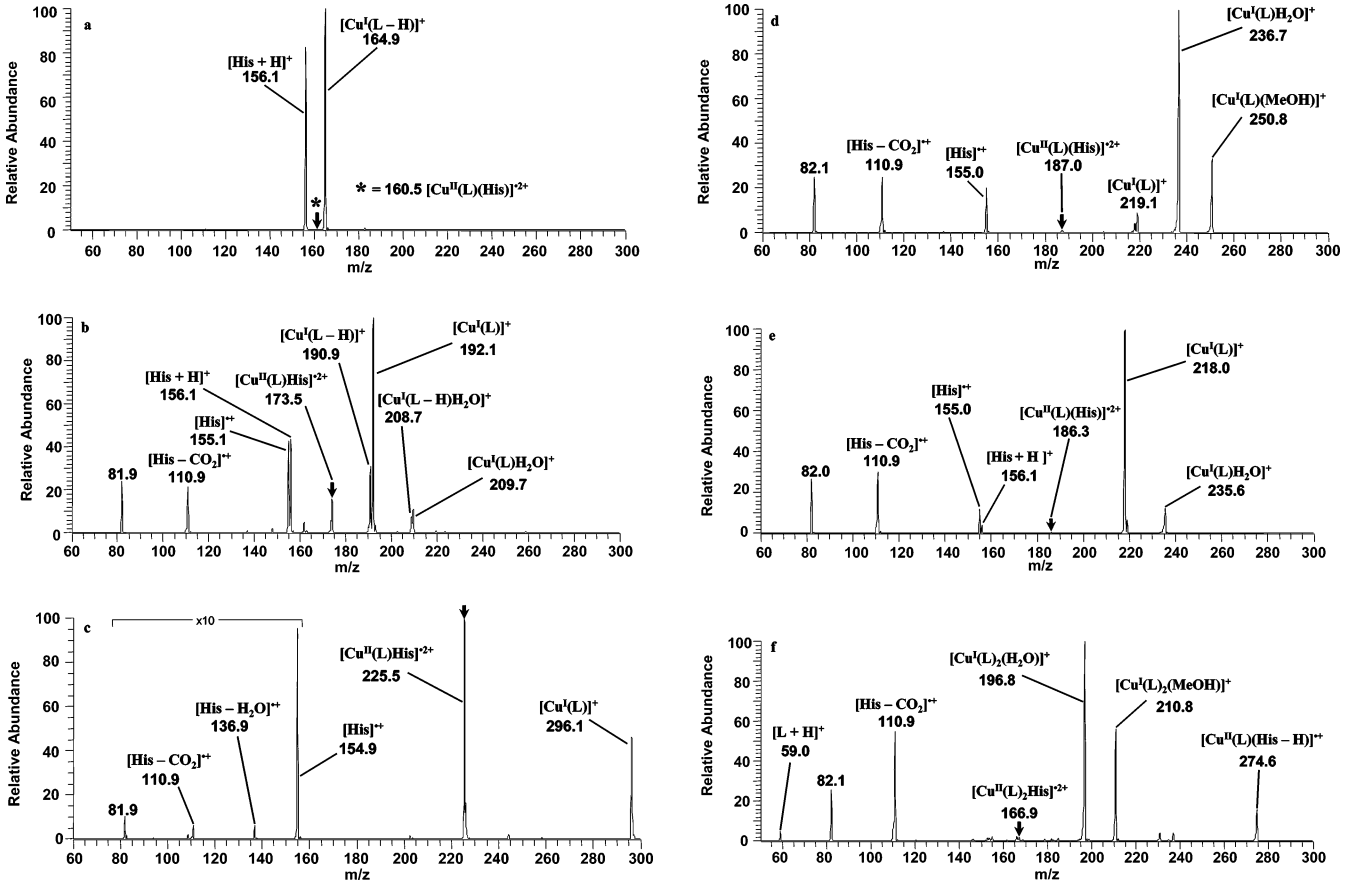

Figure 1. CID spectra of complexes $[Cu^{II}(L)_n(His)]^{\bullet 2+}$ with auxiliary ligand L: (a) dien ($n = 1$), (b) tacn ($n = 1$), (c) tpy ($n = 1$), (d) bpy ($n = 1$), (e) histidine ($n = 1$), and (f) acetone ($n = 2$) at relative collision energies of 8%. The precursor ion is indicated by a bold arrow. The solvated ions were formed as a result of ion−molecule reactions between the product ions and solvent molecules in the trap.

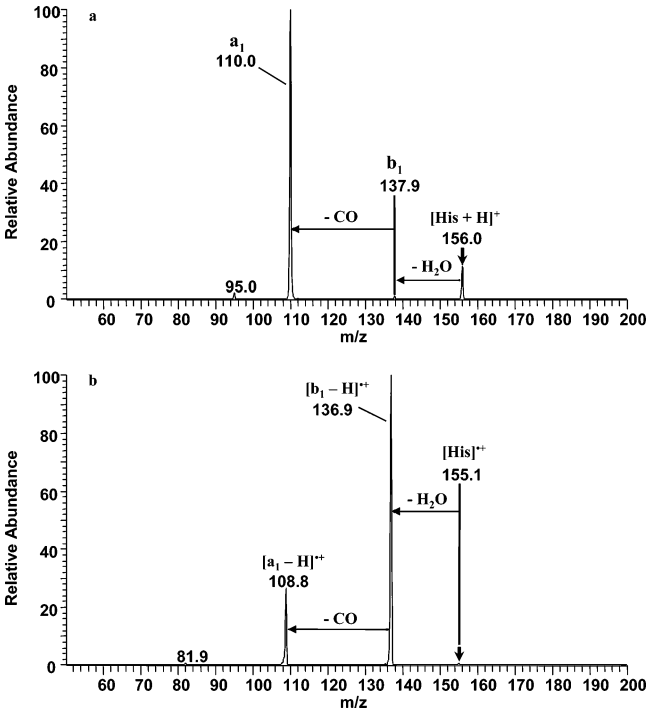

Figure 2. CID spectra of (a) $[His + H]^+$ and (b) $His^{\bullet +}$ at relative collision energies of 10%. The precursor ion is indicated by a bold arrow.

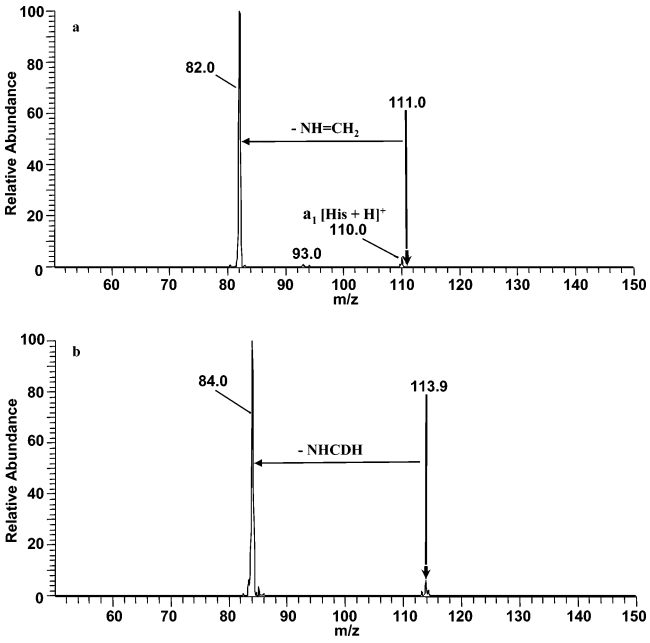

Figure 3. CID of (a) the 111 Th ion and (b) the analogous ion at 114 Th in α,β,β-trideuterated histidine at relative collision energies of 9%. The precursor ion is indicated by a bold arrow. The results in (b) show the loss of d_1-methanimine to give the d_2-4-methyleneimidazole radical cation at 84 Th. See the text for details of the products. The 110 Th ion in panel a is a fragmentation product of protonated histidine, a minor contaminant in the isolation of the 111 Th ion.

a facile loss of ammonia to give $[Cu^{II}(L)(Lys - NH_3)]^{\bullet 2+}$, in accordance with previous observations when tpy[31] and bpy[41,42] were used as auxiliary ligands. Consistent with the fragmentation of protonated lysine,[43−45] ammonia is lost from the side chain, as confirmed by an experiment using ^{15}N-α-amino-labeled lysine

SCHEME 1: Fragmentation Channels of $[Cu(L)_n(His)]^{\bullet 2+}$

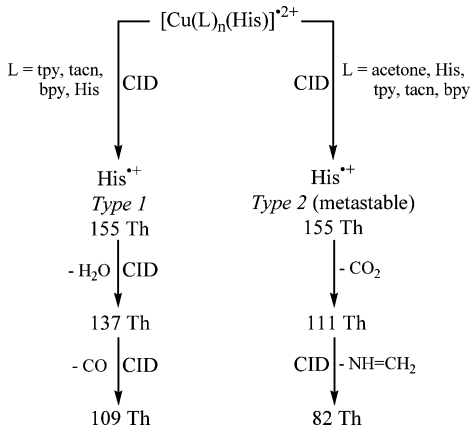

SCHEME 2: Possible Pathways for the Generation of Type 1 and Type 2 Histidine Radical Cations through Rearrangement of a Common Precursor (A) or Separate Formation of Two Different Radical Cations (B)

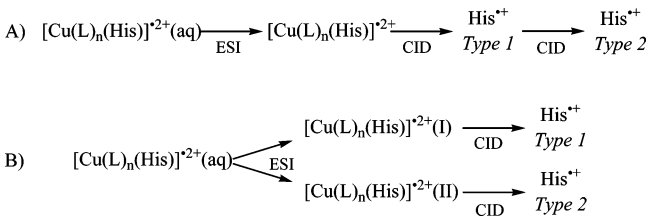

SCHEME 3: Possible Cu^{II}−Histidine Coordination Modes; Bidentate Zwitterionic (1, 2), Bidentate Canonical (3), Monodentate Zwitterionic (4), and Monodentate Canonical (5)

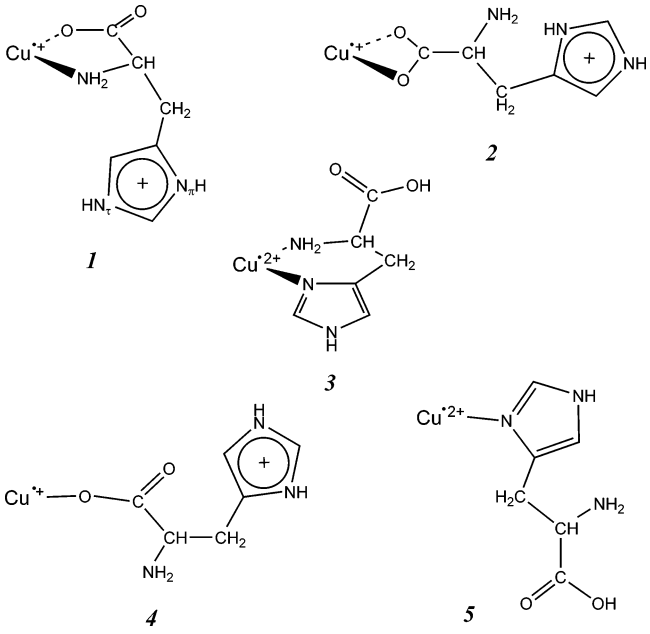

(Figure 4d). In addition to the stable, Type 1, radical cation of lysine at 146 Th, ions at 102 Th and 85 Th are also present in low abundance (Figure 4c), which shift to 103 Th and 86 Th for the ^{15}N-α-amino-labeled lysine (Figure 4d); this establishes that the unlabeled side chain amino group is eliminated as ammonia, probably through nucleophilic displacement by the labeled α-amino group, as in the loss of ammonia in the CID of protonated lysine.[43−45]

When acetone was used as the auxiliary ligand, the abundance of Type 2 ions increased (as demonstrated by relatively high abundances of the 102 Th and 85 Th ions) and the Type 1 ions were in extremely low abundance (Figure 4e). These observations were analogous to those for the histidine complexes. Furthermore, as with the Type 1 ion for histidine, CID of the lysine radical cation at 146 Th resulted in the loss of H_2O as the major fragmentation channel (see Supporting Information, Figure 1S), with notable absence of fragmentation products at 102 Th and 85 Th. The CID of protonated lysine does not generate 102 and 85 Th ions. As before for histidine, we have therefore concluded that these ions originate from the dissociation of metastable Type 2 radical cations of lysine.[45]

The CID spectra of $[Cu^{II}(L)(Arg)]^{\bullet 2+}$ (L = tacn, bpy) show a trace of the Type 1 radical at 174 Th (Figure 5a,b). Using arginine as the auxiliary ligand, the ion at 174 Th is clearly evident (Figure 5c), but is absent when L = acetone (Figure 5d). However, the ion at 130 Th, generated by the loss of CO_2 from the Type 2 arginine radical cation, is always unambiguously present for all complexes examined. Isolation and CID of the stable, Type 1 arginine radical cation (174 Th, Figure 1S in Supporting Information), did not yield the 130 Th fragment, but instead resulted in an ion at 87 Th, reported to be the ethylguanidine radical cation.[31] This behavior is similar to that of the arginine radical cation produced by the CID of $[Fe^{III}(salen)(Arg)]^{\bullet +}$, in which formation of the captodative radical, $(H_2N)_2C^+NH(CH_2)_3C^{\bullet}(NH_2)(COOH)$, was postulated, followed by the loss of dehydroalanine.[31] The behavior of the metastable, Type 2 radical cation of arginine was similar to that of histidine and lysine, effectively preventing direct observation by losing CO_2 rapidly to form a stable ion at 130 Th. This type of fragmentation has been reported by Gatlin et al.[42] using $[Cu^{II}(bpy)(Arg)]^{\bullet 2+}$ and is further supported by recent observations by Barlow et al.[31] using $[Cu^{II}(tpy)(Arg)]^{\bullet 2+}$.

For all the complexes involving basic amino acids examined here, when acetone was the auxiliary ligand, decomposition products of the metastable, Type 2 radical cations were essentially the only products. In contrast, when tpy was the auxiliary ligand, formation of the stable, Type 1 radical cations was favored. Table 1 shows the ratios of abundances for Type 1/Type 2 histidine ions for the various auxiliary ligands. The calculated bond dissociation energies of the $[Cu(L)]^{\bullet 2+}$ complexes provide a measure of the strength of the interaction between $Cu^{\bullet 2+}$ and the auxiliary ligand L; when the interaction is small, the localized charge on the copper is large, a condition that favors binding histidine as a zwitterion. In subsequent sections, we focus on the chemistry of histidine as the prototypical example, as it exhibits cleaner fragmentation channels and the widest range of variations over a number of auxiliary ligands.

Origin of the Observed Type 1 and Type 2 Radical Cations. The two histidine radical cation isomers can originate from either a common radical cation precursor that rearranges (Scheme 2A), or different precursor radical cations that do not interconvert (Scheme 2B). On the basis of the known metastable character of carboxy-centered radicals,[46,47] we assume that a rearrangement step will not have a carboxy radical as the precursor. If a single imidazole-based radical cation (the precursor of a Type 1 ion) is generated, a hydrogen-atom transfer is required to generate the carboxy-centered radical, a Type 2 ion, that will spontaneously eliminate CO_2. However, as CID of the isolated 155 Th ion does not result in the loss of carbon dioxide, the intermediate rearrangement step from Type 1 to Type 2 can be excluded. Instead, the initial formation of two

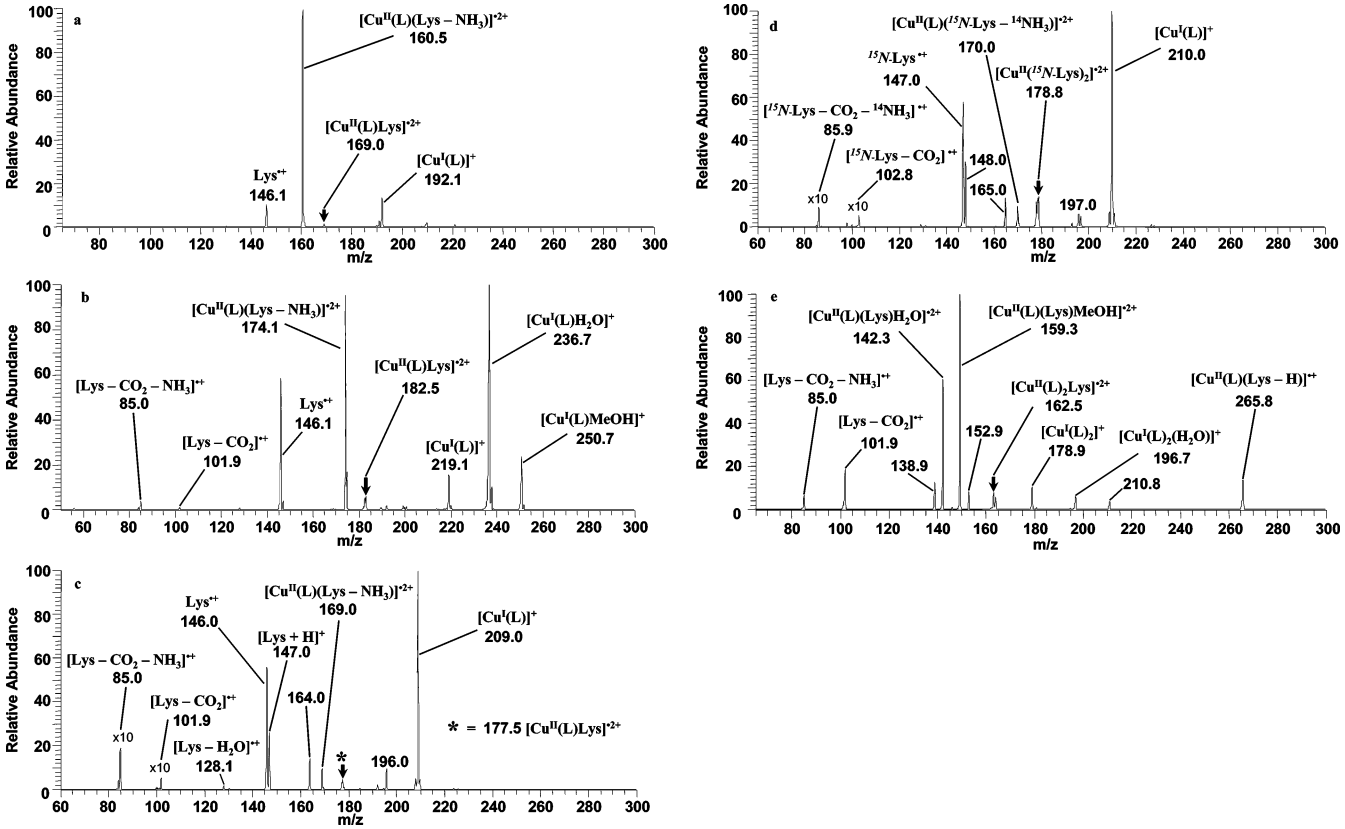

Figure 4. CID spectra of (a) $[Cu^{II}(tacn)(Lys)]^{\bullet 2+}$, (b) $[Cu^{II}(bpy)(Lys)]^{\bullet 2+}$, (c) $[Cu^{II}(Lys)_2]^{\bullet 2+}$, (d) $[Cu^{II}(^{15}N\text{-}Lys)_2]^{\bullet 2+}$, and (e) $[Cu^{II}(acetone)_2(Lys)]^{\bullet 2+}$ at relative collision energies of 7%. The precursor ion is indicated by a bold arrow. Minor fragment ion assignments: (c) 164 Th = $[Cu^{I}(Lys - H) - CO_2]^+$, 196 Th is not assigned; (d) 148 Th = $[^{15}N\text{-}Lys + H]^+$, 165 Th = $[Cu^{I}(^{15}N\text{-}Lys - H) - CO_2]^+$, 197 Th is not assigned; (e) 139 Th = $[Cu^{I}(acetone)(H_2O)]^+$, 153 Th = $[Cu^{I}(acetone)(MeOH)]^+$ (MeOH = methanol), and 211 Th = $[Cu^{I}(acetone)_2(MeOH)]^+$.

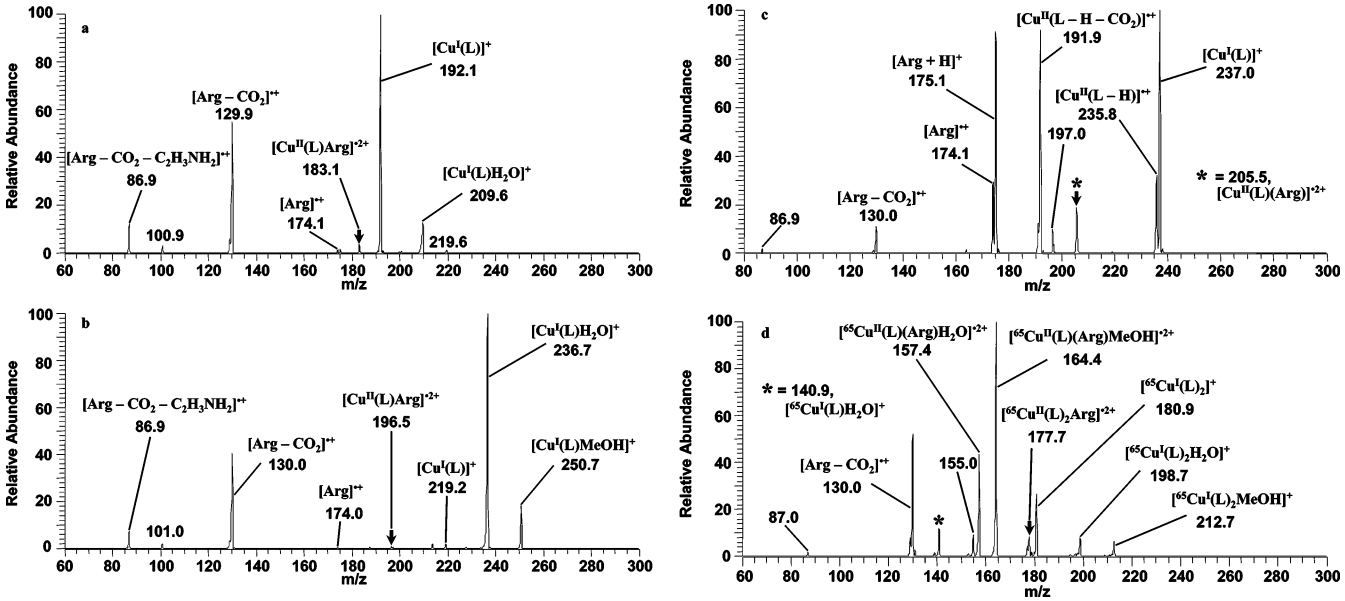

Figure 5. CID of (a) $[Cu^{II}(tacn)(Arg)]^{\bullet 2+}$, (b) $[Cu^{II}(bpy)(Arg)]^{\bullet 2+}$, (c) $[Cu^{II}(Arg)_2]^{\bullet 2+}$, and (d) $[Cu^{II}(acetone)_2(Arg)]^{\bullet 2+}$ at relative collision energies of 8%. The precursor ion is indicated by a bold arrow. Because of the proximity of protonated arginine (176 Th) with $[^{63}Cu^{II}(acetone)_2(Arg)]^{\bullet 2+}$ (176.5 Th), the spectrum shown in panel d is that of the ^{65}Cu complex. Minor fragment ions: (c) 197 Th is not assigned; (d) 155 Th = $[Cu^{I}(acetone)(MeOH)]^+$.

different radical cations is assumed, suggesting strongly that the histidine binding modes to the copper are different.

Histidine Binding Modes. As argued above, different binding modes within the copper(II) complex in the gas phase are proposed to result in the observed Type 1 and Type 2 radical cations. While the binding of zwitterionic histidine might be envisioned as a vestige of the binding of preformed histidine zwitterions in solution, the binding of canonical histidine requires tautomerism and is more difficult to visualize. Recent solution-phase measurements on the coordination behavior of histidine in the Cu^{II}−(bis)histidine complex as a function of pH using infrared (IR), Raman, ultraviolet/visible/near-IR, electron spin resonance, and X-ray absorption spectroscopy indicate that, at all pH values, complexes between histidine and

TABLE 1: Auxiliary Ligand Effects on the Formation of the Two Histidine Radical Cations

complex	*m/z* (Th)	BDE[a] of $[Cu(L)]^{\bullet 2+}$ (kcal/mol)	Type 1/ Type 2[b]	extent of fragmentation (%)
$[Cu^{II}(tpy)(His)]^{\bullet 2+}$	225.5	367.9	6.21	32.0
$[Cu^{II}(tacn)(His)]^{\bullet 2+}$	173.5	326.5	0.98	96.1
$[Cu^{II}(bpy)(His)]^{\bullet 2+}$	187.0	299.2	0.42	99.1
$[Cu^{II}(His)_2]^{\bullet 2+}$	186.5	300.2[c] 305.6[d]	0.21	99.5
$[Cu^{II}(acetone)_2(His)]^{\bullet 2+}$	167.0	288.4[e]	0.03	98.7

[a] BDE: bond dissociation energy, calculated at the B3LYP/6-311++G(d,p) level of theory. [b] Type 1: sum of abundances of 109, 137, and 155 Th; Type 2: sum of abundances of 82 and 111 Th. All ratios were determined at relative collision energies of 8%. [c] BDE of $[Cu^{II}$(zwitterionic His)$]^{\bullet 2+}$ complex. [d] BDE of $[Cu^{II}$(canonical His)$]^{\bullet 2+}$ complex. [e] Elimination of two acetone ligands.

$Cu^{\bullet 2+}$ invariably involve a carboxylate anion; however, as the pH is raised, the Cu−N interaction becomes more dominant.[16,48] At pH 7 and higher, the prevalent complex has no net charge, essentially consisting of two histidine anions coordinated to the $Cu^{\bullet 2+}$ predominantly through two nitrogen atoms (the α-amino and one imidazole N) in a square-planar arrangement, and with one carboxyl oxygen from each histidine coordinating weakly from the axial positions.[16] In our electrospray experiments, the solutions had a pH of about 7. For the $[Cu(His)_2]^{\bullet 2+}$ complexes, whether these contained two zwitterionic histidines (similar to ions that are prevalent in solution at pH 4) or whether the more weakly coordinated carboxyl groups (prevalent at pH 7) were protonated, thus resulting in canonical histidine ligands, each dicoordinated through two nitrogens to the $Cu^{\bullet 2+}$, was impossible to determine.

Analysis of the *gas-phase* binding modes of histidine is complicated as a result of the presence of two nitrogen atoms in the imidazole ring (N_π and N_τ), the amino group (N_{am}) and two carboxyl oxygens (O_c), allowing for mono-, bi-, or tridentate behavior. The complexation behavior of histidine is further modulated by the preference of $Cu^{\bullet 2+}$ for tetracoordination or for distorted pentacoordination.[44,49−51] If a tridentate auxiliary ligand occupies three coordination sites and Cu^{II} maintains a coordination mode of four in the gas phase,[42,49] the coordination modes for the histidine ligand will be curtailed. Assuming monodentate behavior would result in binding of the carboxyl O_c, or imidazole N_π with the copper (Scheme 3, structures **4** or **5**, respectively). Extension of the copper coordination to five[50,51] would allow the formation of a five-membered chelate ring on histidine (Scheme 3, structure **1**), as observed in the solid state,[6] solution,[16,52] and gas phases.[42,49,52,53] Coordination of the carboxyl group through η^2 interaction (Scheme 3, structure **2**)[54,55] is calculated to be the energetically most favorable complexation mode to $Cu^{\bullet 2+}$ in the gas phase for a single glycine ligand; however, calculations on ternary $[Cu^{II}$(bpy)(amino acid)$]^{\bullet 2+}$ complexes, where the amino acid is leucine, isoleucine, or lysine, indicate a preference for a $N_{am}O_c$ five-membered chelate ring (Scheme 3, structure **1**).[41]

The histidine in structures **1**, **2**, and **4** is zwitterionic and, in the presence of a weak auxiliary ligand, e.g., acetone, will feature more prominently in delocalizing the dipositive charge away from the copper. By comparison, the histidine in structures **3** and **5** is uncharged (canonical) and is, therefore, less effective in delocalizing copper's dipositive charge. In the presence of a strong auxiliary ligand, e.g., tpy, this relative weakness of canonical histidine may be inconsequential as the auxiliary ligand itself is effective in stabilizing the formally dipositive charge on the copper. The effect of copper's charge on the amino acid structure is illustrated by contrasting Cu^+/glycine with $Cu^{\bullet 2+}$/glycine: in the former, the complex with canonical glycine is approximately 10 kcal/mol lower in free energy than the one with zwitterionic glycine,[56−58] a trend opposite to that observed in $Cu^{\bullet 2+}$/glycine.[54,55] To gain insight into the energetics of some of the ternary complexes being examined here, we performed DFT calculations. The lowest-energy structures are shown in Figure 6. For complexes in which the auxiliary ligand is tpy, which contributes three strong Cu-binding sites, Cu−His binding involves one strong and one weak bond. In **TC1**, the zwitterionic His binds Cu primarily with one of its carboxy oxygens; there is a weak interaction between Cu and the amino nitrogen, but the bond distance (2.445 Å) is long. Similarly, in **TC2**, the canonical His binds Cu primarily with its imino nitrogen on the side chain; the Cu−amino N distance is long. Thus, in both structures, the contribution of N_{am} to copper-binding is limited. The calculated enthalpy difference between the two $[Cu^{II}(tpy)(His)]^{\bullet 2+}$ complexes is only 0.1 kcal/mol (see Supporting Information, Table 1S).

For complexes in which the auxiliary ligands are two acetones, which contribute only a total of two Cu-binding sites, Cu-His binding involves two bonds of comparable distances and, presumably, strength. In **AC1**, Cu is dicoordinated by a carboxy oxygen and the amino nitrogen of zwitterionic His. This is to be compared with **AC2**, in which Cu is also dicoordinated, but by the imino nitrogen on the side chain and the amino nitrogen of canonical His; there is also a weaker third interaction between Cu and the carbonyl oxygen. **AC1** is lower in enthalpy than **AC2** by 4.0 kcal/mol (see Supporting Information, Table 1S, for details). Acetone as the auxiliary ligand, therefore, favors $N_{am}-O_c$ binding of the zwitterionic form of histidine to copper in the gas phase. In contrast, with tpy as the auxiliary ligand, the binding energies of the canonical and zwitterionic histidine forms are almost identical, favoring the canonical structure by only 0.1 kcal/mol, which is smaller than the expected accuracies of ≤2−3 kcal/mol for DFT calculations.[59,60] Thus these results for the $[Cu^{II}(tpy)(His)]^{\bullet 2+}$ complexes are too close to energetically determine which structure predominates in the gas phase or whether both structures can be present in comparable abundances. Calculations on the dissociation barriers are more revealing. Dissociating the complexes to $[Cu^{I}(tpy)]^+$ and $His^{\bullet +}$ by lengthening the Cu−His bonds while freezing all other bond distances and angles to produce the dissociation products allows us to estimate the dissociation barriers. These are the upper limits, as the "transition states" and the final product structures are reactant-like; we, however, envision that the errors will only be +2−4 kcal/mol. (Freezing the structures was the only solution that worked for the otherwise intractable problem due to the size of the complexes and conformational changes in the incipient $His^{\bullet +}$.) The barrier against dissociating **TC2** (38.1 kcal/mol) is larger than the barrier against dissociating **TC1** (32.7 kcal/mol) by 5.4 kcal/mol. This means that the $[Cu^{II}(tpy)(His)]^{\bullet 2+}$ complex containing canonical His is kinetically more stable than the complex containing zwitterionic His.

Comparison between Experiments and Theory. Results of the DFT calculations for $[Cu^{II}(acetone)_2(His)]^{\bullet 2+}$ are in accord with experimental observations. DFT calculations show that the complex containing zwitterionic histidine bound to Cu^{II} via $N_{am}-O_c$ binding has the lowest energy and should, therefore, comprise the vast majority of $[Cu^{II}(acetone)_2(His)]^{\bullet 2+}$ isolated for CID. Dissociative electron transfer would yield the Type 2 $His^{\bullet +}$ ions, consistent with the experimental data shown in Figure 1f. For $[Cu^{II}(tpy)(His)]^{\bullet 2+}$, DFT calculations show that the complex containing zwitterionic histidine and that containing

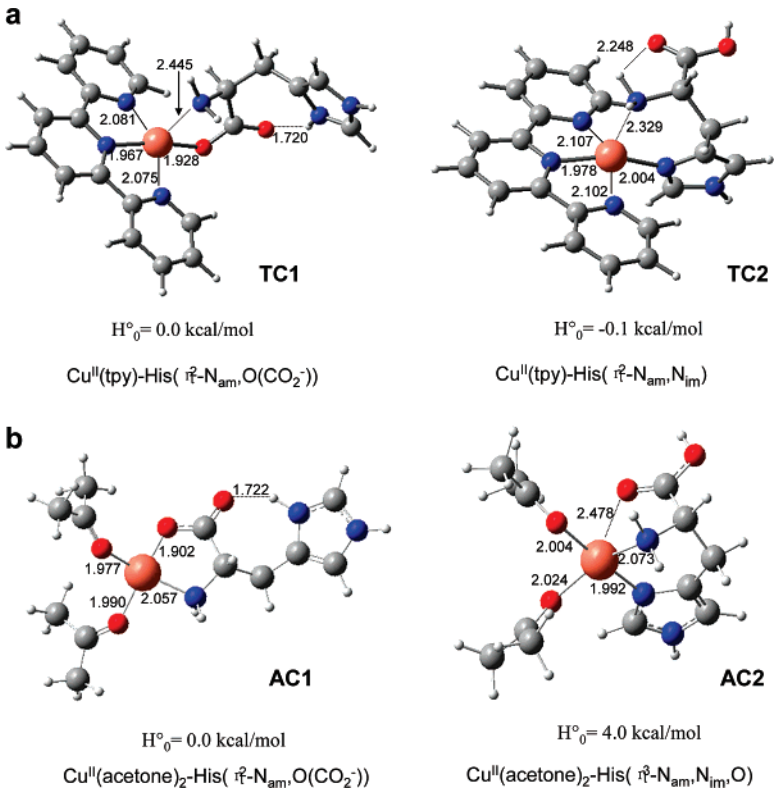

Figure 6. Lowest-energy structures of (a) $[Cu^{II}(tpy)(His)]^{\bullet 2+}$ (**TC1** and **TC2**) and (b) $[Cu^{II}(acetone)_2(His)]^{\bullet 2+}$ (**AC1** and **AC2**) calculated at B3LYP/6-311++G(d,p).

canonical histidine are of similar energy, but the former is kinetically less stable than the latter. Experimentally, the dissociation of $[Cu^{II}(tpy)(His)]^{\bullet 2+}$ produces predominantly the Type 1 $His^{\bullet +}$ ions (Figure 1c), which indicates a higher abundance of the canonical His-containing complex. We interpret this observation to mean that the complex containing canonical His has, in reality, an even lower relative enthalpy than that given by our DFT calculations and/or that the isolation of the $[Cu^{II}(tpy)(His)]^{\bullet 2+}$ for CID favors the canonical complex due to its higher relative stability.

Structures and Fragmentation Mechanisms of Histidine Radical Cations. DFT calculations were employed in a systematic examination of the structures and relative energies of the histidine radical cation. This task was quite complicated and time-consuming, as each of the five plausible tautomers has a large number of conformers at local minima. We examined two groups of structures: canonical and distonic ions. In studying these structures, one stabilizing feature emerged: for any given tautomer, the structure with the largest number of hydrogen bonds almost invariably has the lowest energy. Structures **His1** to **His5** (see Figure 7) were found to be the lowest-energy tautomers. The canonical structure, **His1**, an aromatic π-radical formed by the removal of an electron from the lowest energy conformer of neutral histidine, has the majority of the charge and spin on the imidazole ring. **His1** could readily be formed by dissociation of **AC2** and **TC2** (Figure 6). Calculations on the model complex $Cu^{\bullet 2+}$−imidazole (in which there is C_s symmetry) showed that dissociation leads directly to the π-radical of imidazole, i.e., in the dissociation, the two σ-electrons initially in the dative bond from N to Cu are retained by the nitrogen of imidazole$^{\bullet +}$, and one of the 6π-electrons of the imidazole is transferred to reduce $Cu^{\bullet 2+}$ to Cu^{+}. **His1** is a possible candidate for the structure of the Type 1 histidine radical cation, albeit the barriers against its rearrangement to **His4** or, more likely, **His5**, the structure at the global minimum, are low. The energies of all structures in Figure 7 are reported relative to that of **His1**.

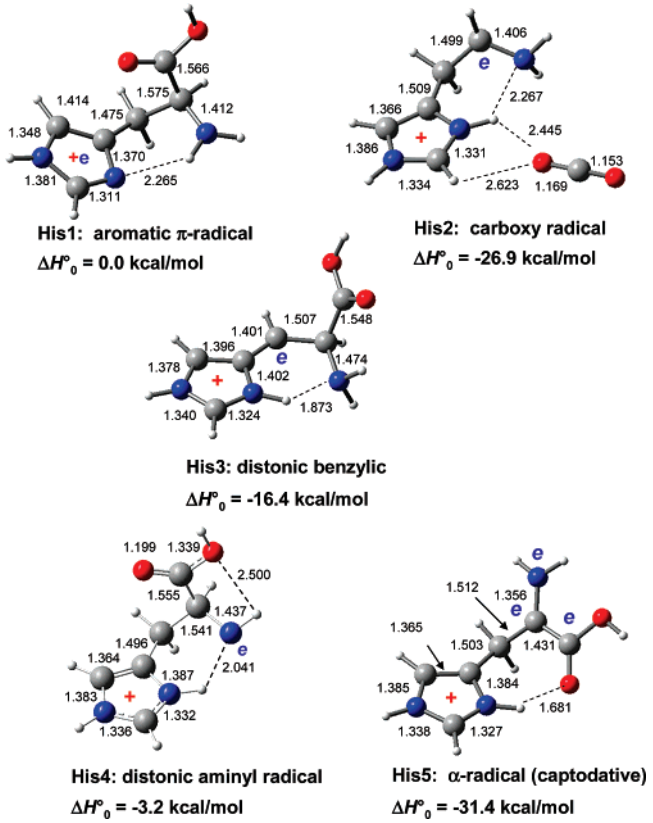

Figure 7. Lowest-energy tautomers of $His^{\bullet +}$ optimized at the B3LYP/6-311++G(d,p) level of theory.

Distonic ions[61−64] are open-shell species in which the spin and charge are formally located on different centers; these ions

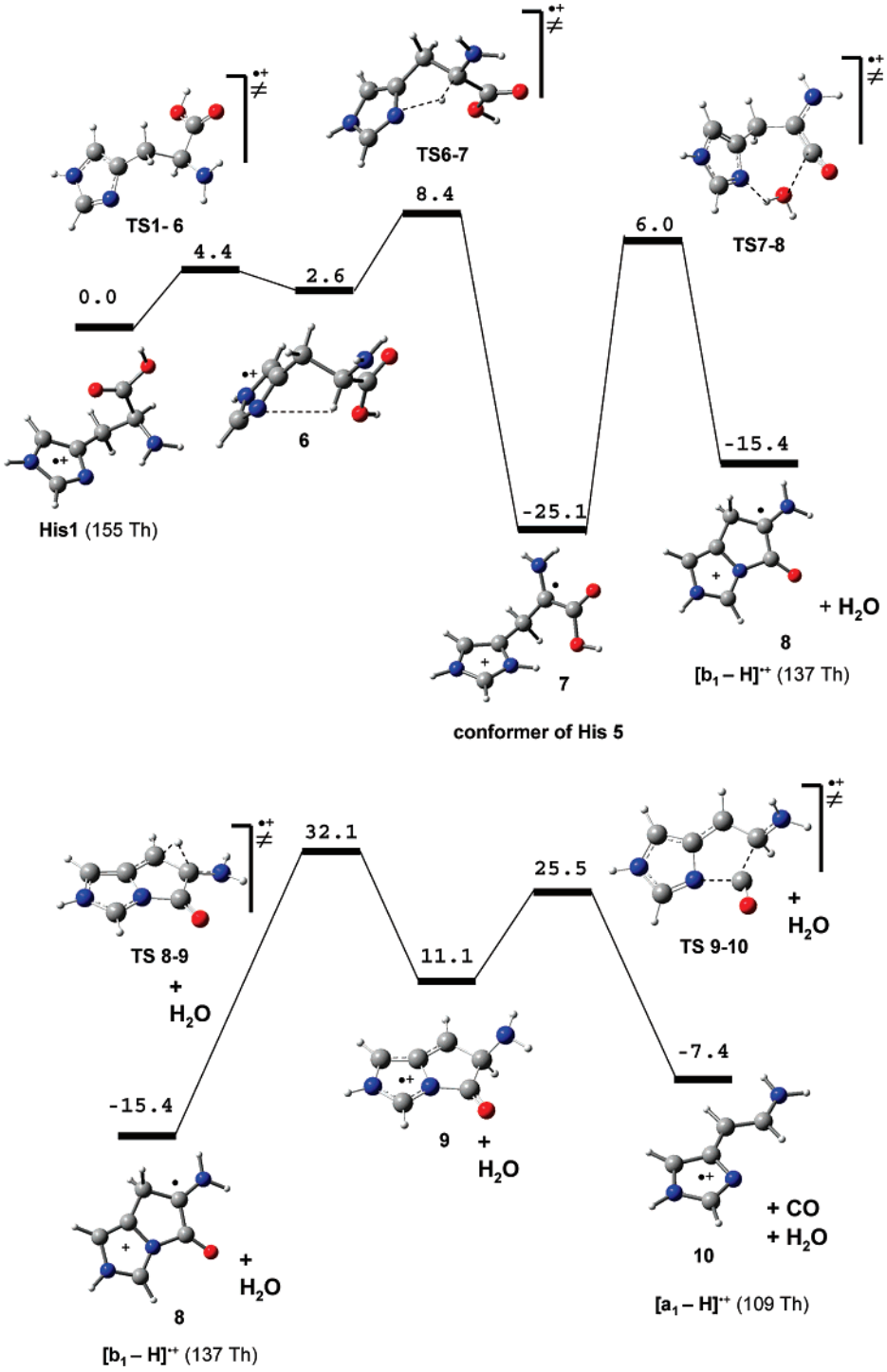

Figure 8. Potential-energy surface for the dissociation of **His1** to give the $[b_1 - H]^{\bullet +}$ ion and subsequently the $[a_1 - H]^{\bullet +}$ ion at the B3LYP/6-311++G(d,p) level of theory. All values are ΔH°_0 in kcal/mol.

are often thermodynamically more stable than isomeric canonical cation-radicals in which an electron has been removed from either a lone pair or a delocalized π-system. **His2**−**His5** are all distonic ions that have energies lower than that of canonical **His1**. **His2** is a carboxy radical created by the migration of a hydrogen from the carboxylic group to the N_π imidazole nitrogen; it is lower in energy than **His1** by 26.9 kcal/mol. At lower levels of theory, **His2** has an intact $C_\alpha - CO_2$ bond; however, at B3LYP/6-311++G(d,p), the only carboxy radical structure at a minimum has the CO_2 molecule loosely solvating the 4-ethaniminoimidazole radical cation, a distonic ion in which the imidazole is protonated and the radical center is on the α-carbon (adjacent to the NH_2 group). Loss of CO_2 from this solvated ion is endothermic by only 3.4 kcal/mol. Consequently, **His2** is too fragile to be isolated experimentally (*vide supra*), and appears to be the metastable, Type 2 radical cation. **His3** is a benzylic-like radical in which the charge is delocalized over the imidazole ring and the spin is largely on the exocyclic (β) carbon; this distonic ion is lower in energy than **His1** by 16.4 kcal/mol. Another distonic structure, **His4**, an aminyl radical cation that can be formed from **His1** via a 1,5 H-shift from the amino group to the ring imino nitrogen, is 3.2 kcal/mol lower in energy than His1. Conversion of **His1** to **His4** has a low barrier, calculated by Barlow et al. to be only 1.7 kcal/mol at the B3LYP/6-31G(d) level.[31] The barrier that we obtained at the B3LYP/6-311++G(d,p) level is 2.2 kcal/mol.

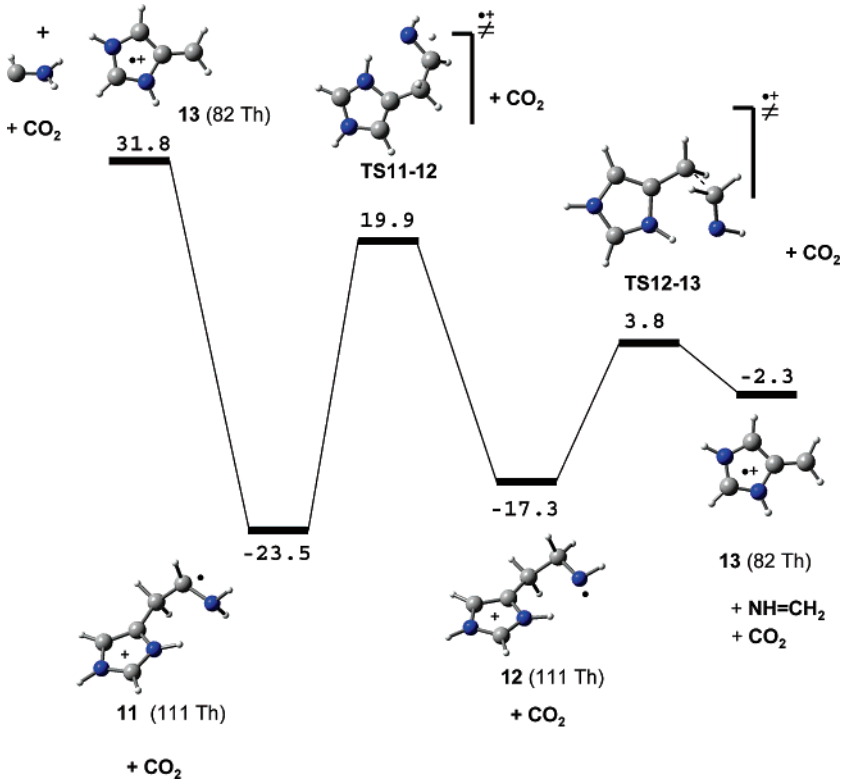

Figure 9. Potential-energy surface for the dissociation of the 4-ethaniminoimidazole radical cation, structure **11**, formed by the loss of CO_2 from **His2** at the B3LYP/6-311++G(d,p) level of theory. All values are ΔH°_0 in kcal/mol.

The tautomer at the global minimum, **His5**, is lower in energy than **His1** by 31.4 kcal/mol. **His5** is an α-carbon-centered radical with both an adjacent π-donor (NH_2) and π-acceptor (COOH). A radical having such a property is described as captodative[20,65−68] and has high stability. In **His5**, the proton is located on the strongly basic imidazole ring and is involved in a strong hydrogen bond to the carbonyl oxygen ($N_{im}H^+\cdots O_c$ = 1.681 Å). This effectively transfers a large amount of positive charge onto the carboxy group, thereby enriching the π-accepting ability of the COOH group, which in turn enhances the stabilization due to the captodative effect. The radical site is delocalized with spin densities of 0.44, 0.29, and 0.16 on the α-C, NH_2, and carbonyl oxygen, respectively.

The stable, Type 1, $His^{\bullet+}$ ion that is sufficiently stable to survive isolation and is available for subsequent CID loses water at lower collision energies and then CO at higher collision energies. This combination of losses is common to all protonated amino acids, although the losses are typically concomitant owing to the instability of the intermediate acylium ion.[44,69,70] The ion produced by the initial loss of water from $His^{\bullet+}$ ion must, therefore, have some inherent stabilizing factor, probably resulting from trapping of the acylium ion by binding to the imidazole nitrogen and forming a bicyclic ion. Removal of a water molecule from **His3** and **His4** would give ions that are distonic, but not captodative. In contrast, **His1** rearranges with a low barrier to **His5**; the $[b_1 - H]^{\bullet+}$ ion (structure 8, Figure 8), a stable captodative radical cation, is formed by removal of water from a rotamer of **His5** (structure 7).

Figure 8 shows the potential energy surface of the proposed reaction mechanism. Starting from the aromatic π-radical **His1**, the first step involves rotation about the $C_\alpha-C_\beta$ bond leading to another conformer, structure **6**, in which the α-carbon hydrogen interacts weakly with the imidazole nitrogen. Structure **6** is higher in energy than **His1** by 2.6 kcal/mol, and the barrier against its formation is 4.4 kcal/mol. In the second step, the α-carbon hydrogen atom is transferred to the imidazole nitrogen via **TS6−7** to produce the stable captodative radical cation **7**, a conformer of **His5**; this step has a barrier of 8.4 kcal/mol (relative to **His1**). The ensuing step, migration of a proton from the imidazole nitrogen to the OH group, followed by the loss of a H_2O molecule via **TS7−8** has a barrier of 6.0 kcal/mol (relative to **His1**), 2.4 kcal/mol lower than that of the preceding step. Starting with **His1** then, the overall barrier to water loss by this mechanism is 8.4 kcal/mol, 5 kcal/mol lower than that previously reported.[31] Overall, the fragmentation reaction to form the $[b_1 - H]^{\bullet+}$ ion (m/z = 137) by the loss of H_2O is exothermic by 15.4 kcal/mol. The stability of the $[b_1 - H]^{\bullet+}$ ion is attributed to its captodative character: the radical center on the α-carbon is flanked by (1) a carbonyl group attached to the positively charged imidazole, making it strongly electron-withdrawing, and (2) the amino group, a powerful electron donor. The loss of CO to generate the $[a_1 - H]^{\bullet+}$ ion involves a 1,2-H shift via **TS8−9** to form structure **9** with a barrier of 47.5 kcal/mol relative to $[b_1 - H]^{\bullet+}$; the subsequent elimination of CO via **TS9−10** has a barrier of 40.9 kcal/mol relative to $[b_1 - H]^{\bullet+}$. This proposed mechanism is consistent with the observed stability of the $[b_1 - H]^{\bullet+}$ ion (137 Th) under CID conditions (Figure 2b). The final products, $[a_1 - H]^{\bullet+} + H_2O + CO$, lie 7.4 kcal/mol below **His1**.

As discussed above, the metastable, Type 2, carboxy radical **His2** readily loses CO_2 to produce the 4-ethaniminoimidazole radical cation at 111 Th (structure **11**). The reaction profile for forming the 4-methyleneimidazole radical cation at 82 Th (structure **13**) from ion **11** is given in Figure 9. The loss of methanimine, $NH{=}CH_2$, is endothermic by 21.2 kcal mol^{-1}, but with a barrier of 43.4 kcal/mol (**TS11−12**) as a result of the required 1,2-H shift from the amino nitrogen to the α-carbon. This barrier against the loss of methanimine is 11.9 kcal/mol lower than that against the direct loss of aminocarbene, NH_2-CH (which is endothermic by 55.3 kcal/mol). The facile loss

of CO_2 and the existence of the barrier against the loss of NH═CH_2 support the assignment of **His2** as the Type 2 radical cation in Scheme 1 and is consistent with experimental observation (Figures 1 and 3).

There is experimental evidence that some of the 4-methyleneimidazole radical cations, especially under relatively high collision energies, can be formed directly from dissociation of the $[Cu^{II}(L)_n(His)]^{\bullet 2+}$ complex. Indeed, as an example, the barrier against this direct dissociation from **TC1**, the $[Cu^{II}(tpy)(His)]^{\bullet 2+}$ complex containing zwitterionic His, is only at 45.3 kcal/mol.

Conclusions

CID of complexes $[Cu(L)(M)]^{\bullet 2+}$, where M is a basic amino acid, produces two types of radical cations: Type 1 ions that are stable on the mass spectrometry time scale, and Type 2 ions that are too unstable to detect directly, but are observable as $[M - CO_2]^{\bullet +}$. The auxiliary ligand, L, plays a key role in determining which type of radical cation is formed predominantly. For complexes that contain a strong auxiliary ligand, Type 1 ions are produced preferentially to Type 2 ions, whereas, for those that contain a weak auxiliary ligand, Type 2 ions are produced. The Type 1 histidine radical ion is probably formed as a π-radical, **His1**, but there is a low barrier of only 8.4 kcal/mol against conversion to the lowest energy tautomer, **His5**. This latter tautomer has remarkable stability due to its captodative character. The Type 2 histidine radical ion is probably a carboxy radical with the charge located on the imidazole ring, **His2**, which is best described as a distonic protonated imidazole ion solvated by CO_2. **His2** is only metastable, as the elimination of CO_2 has a barrier of only 3.4 kcal/mol.

Acknowledgment. This research is supported by the Natural Sciences and Engineering Research Council (NSERC) of Canada and MDS SCIEX. We thank the Shared Hierarchical Academic Research Computing Network, SHARCNET, for providing a part of the computational resources and time. Y.K. acknowledges receipt of an Ontario Graduate Scholarship.

Supporting Information Available: Tables of relative enthalpies, relative free energies, total energies, Cartesian coordinates of the various $[Cu^{II}(\text{auxiliary ligand})_nHis]^{\bullet 2+}$ complexes, and CID spectra. This material is available free of charge via the Internet at http://pubs.acs.org.

References and Notes

(1) Kozlowski, H.; Bal, W.; Dyba, M.; Kowalik-Jankowska, T. *Coord. Chem. Rev.* **1999**, *184*, 319−346.
(2) Anbalagan, V.; Van Stipdonk, M. J. *J. Mass Spectrom.* **2003**, *38*, 982−989.
(3) Sinz, A.; Jin, A. J.; Zschornig, O. *J. Mass Spectrom.* **2003**, *38*, 1150−1159.
(4) Miura, T.; Satoh, T.; Hori-i, A.; Takeuchi, H. *J. Raman Spectrom.* **1998**, *29*, 41−47.
(5) Gaggelli, E.; D'Amelio, N.; Valensin, D.; Valensi, G. *Magn. Reson. Chem.* **2003**, *41*, 877−883.
(6) Graham, B.; Hearn, M. T. W.; Spiccia, L.; Skelton, B. W.; White, A. H. *Aust. J. Chem.* **2003**, *56*, 1259−1261.
(7) Parac, T. N.; Ullmann, G. M.; Kostić, N. M. *J. Am. Chem. Soc.* **1999**, *121*, 3127−3135.
(8) Varnagy, K.; Sovago, I.; Suli-Vargha, H.; Sanna, D.; Micera, G. *J. Inorg. Biochem.* **2000**, *81*, 35−41.
(9) Cerda, B. A.; Cornett, L.; Wesdemiotis, C. *Int. J. Mass Spectrom.* **1999**, *193*, 205−226.
(10) Zhao, F.; Ghezzo-Schöneich, E.; Aced, G. I.; Hong, J.; Milby, T.; Schöneich, C. *J. Biol. Chem.* **1997**, *272*, 9019−9029.
(11) Liu, S.; Howlett, G.; Barrow, C. J. *Biochem.* **1999**, *38*, 9373−9378.
(12) Parraga, G.; Horvath, S. J.; Eisen, A.; Taylor, W. E.; Hood, L.; Young, E. T.; Klevit, R. E. *Science* **1988**, *241*, 1489−1492.
(13) Jeuken, L. J. C.; van Vliet, P.; Verbeet, M. P.; Camba, R.; McEvoy, J. P.; Armstrong, F. A.; Canters, G. W. *J. Am. Chem. Soc.* **2000**, *122*, 12186−12194.
(14) Ferguson-Miller, S.; Babcock, G. T. *Chem. Rev.* **1996**, *96*, 2289−2907.
(15) Casella, L.; Gulloti, M. J. *Inorg. Biochem.* **1983**, *18*, 19−31.
(16) Mesu, J. G.; Visser, T.; Soulimani, F.; van Faassen, E. E.; dePeinder, P.; Beale, A. M.; Weckhuysen, B. M. *Inorg. Chem.* **2006**, *45*, 1960−1971.
(17) Chu, I. K.; Rodriquez, C. F.; Lau, T. C.; Hopkinson, A. C.; Siu, K. W. M. *J. Phys. Chem. B* **2000**, *104*, 3393−3397.
(18) Chu, I. K.; Rodriquez, C. F.; Hopkinson, A. C.; Siu, K. W. M.; Lau, T. C. *J. Am. Soc. Mass Spectrom.* **2001**, *12*, 1114−1119.
(19) Bagheri-Majdi, E.; Ke, Y.; Orlova, G.; Chu, I. K.; Hopkinson, A. C.; Siu, K. W. M. *J. Phys. Chem. B* **2004**, *108*, 11170−11181.
(20) Hopkinson, A. C.; Siu, K. W. M. In *Principles of Mass Spectrometry Applied to Biomolecules*; Laskin, J., Lifshitz, C., Eds.; Wiley-Interscience: New York, 2006; Chapter 9, pp 301−335.
(21) Ke, Y.; Verkerk, U. H.; Shek, P. Y. I.; Hopkinson, A. C.; Siu, K. W. M. *J. Phys. Chem. B* **2006**, *110*, 8517−8523.
(22) Chu, I. K.; Siu, S. O.; Lam, C. N. W.; Chan, J. C. Y.; Rodriquez, C. F. *Rapid Commun. Mass Spectrom.* **2004**, *18*, 1798−1802.
(23) Chu, I. K.; Lam, C. N. W.; Siu, S. O. *J. Am. Soc. Mass Spectrom.* **2005**, *16*, 763−771.
(24) Chu, I. K.; Lam, C. N. W. *J. Am. Soc. Mass Spectrom.* **2005**, *16*, 1795−1804.
(25) Lam, C. N. W.; Siu, S. O.; Orlova, G.; Chu, I. K. *Rapid Commun. Mass Spectrom.* **2006**, *20*, 790−796.
(26) Wee, S.; O'Hair, R. A. J.; McFadyen, W. D. *Int. J. Mass Spectrom.* **2004**, *234*, 101−122.
(27) Barlow, C. K.; Wee, S.; McFadyen, W. D.; O'Hair, R. A. J. *J. Chem. Soc., Dalton Trans.* **2004**, 3199−3204.
(28) Wee, S.; O'Hair, R. A. J.; McFadyen, W. D. *Rapid Commun. Mass Spectrom.* **2002**, *16*, 884−890.
(29) Barlow, C. K.; McFadyen, W. D.; O'Hair, R. A. J. *J. Am. Chem. Soc.* **2005**, *127*, 6109−6115.
(30) Wee, S.; O'Hair, R. A. J.; McFadyen, W. D. *Int. J. Mass Spectrom.* **2006**, *249*−*250*, 171−183.
(31) Barlow, C. K.; Moran, D.; Radom, L.; McFadyen, W. D.; O'Hair, R. A. J. *J. Phys. Chem. A* **2006**, *110*, 8304−8315.
(32) Hu, P.; Loo, J. A. *J. Am. Chem. Soc.* **1995**, *117*, 11314−11319.
(33) Frisch, M. J.; Trucks, G. W.; Schlegel, H. B.; Scuseria, G. E.; Robb, M. A.; Cheeseman, J. R.; Montgomery, J. A., Jr.; Vreven, T.; Kudin, K. N.; Burant, J. C.; Millam, J. M.; Iyengar, S. S.; Tomasi, J.; Barone, V.; Mennucci, B.; Cossi, M.; Scalmani, G.; Rega, N.; Petersson, G. A.; Nakatsuji, H.; Hada, M.; Ehara, M.; Toyota, K.; Fukuda, R.; Hasegawa, J.; Ishida, M.; Nakajima, T.; Honda, Y.; Kitao, O.; Nakai, H.; Klene, M.; Li, X.; Knox, J. E.; Hratchian, H. P.; Cross, J. B.; Bakken, V.; Adamo, C.; Jaramillo, J.; Gomperts, R.; Stratmann, R. E.; Yazyev, O.; Austin, A. J.; Cammi, R.; Pomelli, C.; Ochterski, J. W.; Ayala, P. Y.; Morokuma, K.; Voth, G. A.; Salvador, P.; Dannenberg, J. J.; Zakrzewski, V. G.; Dapprich, S.; Daniels, A. D.; Strain, M. C.; Farkas, O.; Malick, D. K.; Rabuck, A. D.; Raghavachari, K.; Foresman, J. B.; Ortiz, J. V.; Cui, Q.; Baboul, A. G.; Clifford, S.; Cioslowski, J.; Stefanov, B. B.; Liu, G.; Liashenko, A.; Piskorz, P.; Komaromi, I.; Martin, R. L.; Fox, D. J.; Keith, T.; Al-Laham, M. A.; Peng, C. Y.; Nanayakkara, A.; Challacombe, M.; Gill, P. M. W.; Johnson, B.; Chen, W.; Wong, M. W.; Gonzalez, C.; Pople, J. A. *Gaussian 03*, revision D.01; Gaussian, Inc.: Wallingford, CT, 2004.
(34) Becke, A. D. *J. Chem. Phys.* **1993**, *98*, 5648−5652.
(35) Lee, C. T.; Yang, W. T.; Parr, R. G. *Phys. Rev. B* **1988**, *37*, 785−789.
(36) Rulisek, L.; Havlas, Z. *J. Am. Chem. Soc.* **2000**, *122*, 10428−10439.
(37) de Bruin, Th. J. M.; Marcelis, A. T.; Zuilhof, H.; Sudholter, E. J. R. *Phys. Chem. Chem. Phys.* **1999**, *1*, 4157−4163.
(38) Pablo, C.; Isabel, M. M.; Ramon, L.; Tomas, S. *Chem. Phys. Chem.* **2005**, *6*, 344−351.
(39) Gonzales, C.; Schlegel, H. B. *J. Chem. Phys.* **1989**, *90*, 2154−2161.
(40) Lavanant, H.; Hecquet, E.; Hoppilliard, Y. *Int. J. Mass Spectrom.* **1999**, *185*/*186*/*187*, 11−23.
(41) Seymour, J. L.; Tureček, F. *J. Mass Spectrom.* **2002**, *37*, 533−540.
(42) Gatlin, C. L.; Tureček, F.; Vaisar, T. *J. Mass Spectrom.* **1995**, *30*, 1617−1627.
(43) Dookeran, N. N.; Yalcin, T.; Harrison, A. G. *J. Mass Spectrom.* **1996**, *31*, 500−508.
(44) Milne, G. W. A.; Axenrod, T.; Fales, H. M. *J. Am. Chem. Soc.* **1970**, *92*, 5170−5175.
(45) Rogalewicz, F.; Hoppilliard, Y.; Ohanessian, G. *Int. J. Mass Spectrom.* **2000**, *195*/*196*, 565−590.
(46) Schröder, D.; Soldi-Lose, H.; Schwartz, H. *Aust. J. Chem.* **2003**, *56*, 443−451.
(47) Bossio, R. E.; Hudgins, R. R.; Marshall, A. *J. Phys. Chem. B* **2003**, *107*, 3284−3289.

(48) Mesu, J. G.; Visser, T.; Soulimani, F.; Weckhuysen, B. M. *Vib. Spectrosc.* **2005**, *39*, 114−125.
(49) Gatlin, C. L.; Tureček, F.; Vaisar, T. *J. Am. Chem. Soc.* **1995**, *117*, 3637−3638.
(50) Henke, W.; Kremer, S.; Reinen, D. *Inorg. Chem.* **1983**, *22*, 2858−2863.
(51) Pushie, M. J.; Rauk, A. *J. Biol. Inorg. Chem.* **2003**, *8*, 53−65.
(52) Seymour, J. L.; Tureček, F.; Malkov, A. V.; Kocovsky, P. *J. Mass Spectrom.* **2004**, *39*, 1044−1052.
(53) Tao, W. A.; Zhang, D.; Nikolaev, E. N.; Cooks, R. G. *J. Am. Chem. Soc.* **2000**, *122*, 10598−10609.
(54) Pulkkinen, S.; Noguera, M.; Rodriguez-Santiago, L.; Sodupe, M.; Bertran, J. *Chem.—Eur. J.* **2000**, *6*, 4393−4399.
(55) Marino, T.; Russo, N.; Toscano, M. *J. Mass Spectrom.* **2002**, *37*, 786−791.
(56) Hoyau, S.; Ohanessian, G. *J. Am. Chem. Soc.* **1997**, *119*, 2016−2024.
(57) Bertran, J.; Rodriguez-Santiago, L.; Sodupe, M. *J. Phys. Chem. B* **1999**, *103*, 2310−2317.
(58) Shoeib, T.; Rodriquez, C. F.; Siu, K. W. M.; Hopkinson, A. C. *Phys. Chem. Chem. Phys.* **2001**, *3*, 853−861.
(59) Boys, S. F.; Bernardi, F. *Mol. Phys.* **1970**, *19*, 553−566.
(60) Ketvirtis, A. E.; Bohme, D. K.; Hopkinson, A. C. *J. Phys. Chem.* **1995**, *99*, 16121−16127.
(61) Sustmann, R.; Korth, H. G. *Adv. Phys. Org. Chem.* **1990**, *26*, 131−178.
(62) Yates, B. F.; Bouma, W.; Radom, L. *J. Am. Chem. Soc.* **1984**, *106*, 5805−5808.
(63) Yates, B. F.; Bouma, W.; Radom, L. *Tetrahedron* **1986**, *42*, 6225−6234.
(64) Strik, K. M.; Kiminkinen, L. K. M.; Kenttamaa, H. I. *Chem. Rev.* **1992**, *92*, 1649−1665.
(65) Hammerum, S. *Mass Spectrom. Rev.* **1988**, *7*, 123−202.
(66) Bordwell, F. G.; Zhang, X.; Alnajjar, M. S. *J. Am. Chem. Soc.* **1992**, *114*, 7623−7629.
(67) Easton, C. J. *Chem. Rev.* **1997**, *97*, 53−82.
(68) Croft, A. K.; Easton, C. J.; Radom, L. *J. Am. Chem. Soc.* **2003**, *125*, 4119−4124.
(69) Meot-Ner, M.; Field, F. H. *J. Am. Chem. Soc.* **1973**, *95*, 7207−7211.
(70) Leclercq, P. A.; Desiderio, D. *Org. Mass Spectrom.* **1973**, *7*, 515−533.
(71) Tsang, C. W.; Harrison, A. G. *J. Am. Chem. Soc.* **1976**, *98*, 1301−1308.